


# Posture-related stiffness mapping of paraspinal muscles

Maud Creze,<sup>1,2,3</sup>  Dina Bedretdinova,<sup>4</sup> Marc Soubeyrand,<sup>5</sup> Laurence Rocher,<sup>1,3</sup> Jean-Luc Gennisson,<sup>3</sup> Olivier Gagey,<sup>2,5</sup> Xavier Maître<sup>3</sup> and Marie-France Bellin<sup>1,3</sup>

<sup>1</sup>Radiology Department, Bicêtre Hospital, APHP, Kremlin-Bicêtre, France

<sup>2</sup>Complexité, Innovations, Activités Motrices et Sportives, CIAMS (EA4532), Université Paris-Saclay, Orsay, France

<sup>3</sup>Imagerie par Résonance Magnétique Médicale et Multi-Modalités, IR4M, CNRS, Université Paris-Sud, Université Paris-Saclay, Orsay, France

<sup>4</sup>Centre de recherche en Épidémiologie et Santé des Populations, CESP, INSERM, Université Paris-Saclay, Orsay, France

<sup>5</sup>Department of Orthopedics, Bicêtre Hospital, APHP, Kremlin-Bicêtre, France

## Abstract

The paraspinal compartment acts as a bone–muscle composite beam of the spine. The elastic properties of the paraspinal muscles play a critical role in spine stabilization. These properties depend on the subjects' posture, and they may be drastically altered by low back pain. Supersonic shear wave elastography can be used to provide quantitative stiffness maps (elastograms), which characterize the elastic properties of the probed tissue. The aim of this study was to challenge shear wave elastography sensitivity to postural stiffness changes in healthy paraspinal muscles. The stiffness of the main paraspinal muscles (longissimus, iliocostalis, multifidus) was measured by shear wave elastography at the lumbosacral level (L3 and S1) for six static postures performed by volunteers. Passive postures (rest, passive flexion, passive extension) were performed in a first shear wave elastography session, and active postures (upright, bending forward, bending backward) with rest posture for reference were performed in a second session. Measurements were repeated three times for each posture. Sixteen healthy young adults were enrolled in the study. Non-parametric paired tests, multiple analyses of covariance, and intra-class correlations were implemented for analysis. Shear wave elastography showed good to excellent reliability, except in the multifidus at S1, during bending forward, and in the multifidus at L3, during bending backward. Yet, during bending forward, only poor quality was recorded for nine volunteers in the longissimus. Significant intra- and inter-muscular changes were observed with posture. Stiffness significantly increased for the upright position and bending forward with respect to the reference values recorded in passive postures. In conclusion, shear wave elastography allows reliable assessment of the stiffness of the paraspinal muscles except in the multifidus at S1 and longissimus, during bending forward, and in the multifidus at L3, during bending backward. It reveals a different biomechanical behaviour for the multifidus, the longissimus, and the iliocostalis.

**Key words:** low back pain; lumbosacral region; paraspinal muscles; posture; shear modulus; shear wave elastography; skeletal muscle.

## Introduction

The paraspinal muscles (PsM) allow large tri-dimensional motions of the trunk and, at the same time, ensure the stability of the spine. PsM encompass numerous complex and polyarticular muscles, which are ventrally attached to the dorsal part of the posterior arc of the vertebrae, the dorsal

part of the sacrum, and the iliac crest. PsM are sheathed in an inextensible fascia called the thoracolumbar fascia (TLF), with which they constitute the paraspinal myo-fascial compartment (Willard et al. 2012; Creze et al. 2018c). The paraspinal compartment acts as a bone–muscle composite beam of the spine; its efficacy depends on its mechanical properties, and a disorder of the PSM usually contributes to the development or the persistence of low back pain (LBP; Rabischong & Avril, 1965; Mabit & Rabischong, 1996).

Low back pain is commonly associated with increased trunk stiffness, which is evaluated with various mechanical devices (Colloca & Hinrichs, 2005; Brown & McGill, 2010) and increased PsM stiffness, which is commonly probed by medical palpation (Fryer et al. 2004a,b). Stiffness changes

### Correspondence

Maud Creze, Radiology Department, Bicêtre Hospital, APHP, 78 rue du Général Leclerc, 94275 Le Kremlin-Bicêtre Cedex, France.  
E: maud.creze@aphp.fr

Accepted for publication 13 February 2019  
Article published online 22 March 2019

have also been recorded by strain elastography in the multifidus in LBP (Chan et al. 2012). Yet, all these measurements are qualitative and operator-dependent and do not quantify stiffness changes with respect to LBP (Fryer et al. 2004a, b). Hence, they are not routinely used in clinical practice.

Over the last two decades, parametric imaging techniques have been developed to measure the elastic properties of tissues *in vivo* (Levinson et al. 1995; Bercoff et al. 2004). Today, supersonic shear wave elastography (SWE) allows real-time mapping of the shear elastic modulus,  $\mu$ , by the computation of the shear wave velocity upon ultrafast recording of the displacement field (Gennisson et al. 2010, 2013) induced in the targeted tissue by acoustic radiation force (Gennisson et al. 2010, 2013). SWE efficiently addresses (1) the characterization of passive and active muscle forces (Nordez & Hug, 2010; Hug et al. 2015), (2) the determination of the muscle stiffness influences on joint stiffness (Bouillard et al. 2011), and (3) stiffness changes related to muscle damage and disease (Nordez & Hug, 2010; Bouillard et al. 2011; Lacourpaille et al. 2014, 2015; Hug et al. 2015; Creze et al. 2018b).

So far, most studies have been conducted on appendicular and superficial muscles (Bouillard et al. 2012a; Akagi et al. 2015; Chino & Takahashi, 2016; Creze et al. 2018b) because the ultrasound signal is attenuated in deep tissue and the sensitivity of SWE to anisotropy is detrimental to the reproducibility of the measurements in muscles with complex architecture. Given the parallel arrangement of micro- and macroscopic structures, the muscles are mechanically anisotropic and SWE requires matching the orientation of the probe to the main direction of the muscle fibres (Eby et al. 2013). The trunk muscles are flat, large, multipennate, and/or multiceps (Kalimo et al. 1989). With such complex anatomy, it is not possible to define only one fibre direction and to define the orientation of the ultrasound probe accordingly (Hatta et al. 2016b).

However, when careful probe positioning was undertaken, four studies have demonstrated the reliability and the feasibility of stiffness analysis in trunk muscles (MacDonald et al. 2015; Moreau et al. 2016; Creze et al. 2017; Koppenhaver et al. 2018). In the PsM, reliability estimates were even fair to excellent, higher in the multifidus than in ES (Koppenhaver et al. 2018), also higher at the L2–L3 level than at the L4 level (Moreau et al. 2016). The measurement reliability improved during PsM contraction (Koppenhaver et al. 2018). Recently, Masaki et al. (2017) reported significantly higher stiffness in the multifidus in low back pain than in the control group.

The sensitivity and the robustness of the technique could be a challenge with the posture, as the posture is likely to influence PsM stiffness via muscle stretching and contraction (Moreau et al. 2016; Tran et al. 2016). Indeed, as PsM muscles are polyarticular and attached to several vertebrae, ribs and the pelvis, both passive and active (muscle contraction) changes in relative skeletal position, in all special

planes, are likely to load PsM. Stabilization of the spine requires permanent postural adaptation through PsM contraction and stretching regardless of the posture. PsM bulging contained in an inextensible fascia, which occurs during contraction, may also contribute to increasing stiffness in the paraspinal compartment.

Despite the high prevalence of LBP, its pathophysiology remains poorly understood, in particular regarding the role of PsM in the origin and evolution of LBP. We assume that SWE will allow the study of PsM in an objective, quantitative, and reliable manner. Thereafter, PsM stiffness assessment will contribute to building knowledge on the PsM function so as to determine the functional involvement of muscles in LBP and optimize the healthcare of LBP. The purpose of this study was twofold: first, evaluating the sensitivity of PsM SWE to postures and evaluating the influence of these postures onto PsM stiffness; secondly, to assess the feasibility of SWE stiffness measurements in the main PsM (multifidus, longissimus, and iliocostalis) in healthy adults.

## Materials and methods

### Volunteers

Sixteen healthy, right-handed volunteers were recruited (nine females, seven males; age:  $26.1 \pm 4.9$  years; body mass index (BMI):  $21.3 \pm 2.1 \text{ kg m}^{-2}$ ). The participants were either sedentary ( $n = 11$ ) or physically active ( $n = 5$ ) and did not have a history of chronic back pain that required time off work or treatment. They were asked to refrain from strenuous exercise 48 h before testing. Participants have been properly instructed in the nature of the study before providing a written informed consent. The local ethics committee approved the study protocol, consistent with the Declaration of Helsinki.

### Materials

The shear wave velocity (SWV) was measured in the PsM by using an Aixplorer® ultrasound scanner (SuperSonic Imagine, Aix-en-Provence, France) and a convex probe (SuperCurved 6-1, SuperSonic Imagine). The scanner was used in the general preset 'penetration' mode, which improved the depth of penetration of the shear waves. A generous amount of coupling gel was applied to the surface of the skin so that the tissues were not compressed by the probe while ensuring a good contact. The probe was aligned along the direction of the muscle fibres, as confirmed by B-mode images. The probe was kept motionless during acquisition until the elasticity map stabilized (between 5 and 15 s).

### Experimental protocol

The same operator (10 years' experience in radiology) performed all ultrasound examinations.

Volunteers were asked to perform two passive static postures in a given order during session 1 and, a week later, three active static postures during session 2 (Fig. 1 and S1). Before the beginning of each session, the participant lay in a prone position for 5 min to rest the PsM. A reference stiffness measurement was recorded.

#### Session 1: passive postures (day 1)

- Rest 1: The participant was positioned prone on a folding table with their arms in a neutral anatomical position.
- Passive flexion (30°): The participant lay prone. Passive flexion was performed using a 30° angulation of the examination table at the level of anterior superior iliac spines (ASIS), which were determined by palpation.
- Passive extension (30°): The participant lay prone. Passive extension was performed using a 30° angulation of the examination table at the level of ASIS after 5 min rest (same position as rest 1).

#### Session 2: active postures (day 8)

- Rest 2: The participant was positioned prone on an examination table with their arms in a neutral anatomical position (same as rest 1).
- Upright: Upright position was performed in a neutral upright posture (as perceived by the participant).
- Bending forward (30°): After 5-min rest (same position as rest 2), active 30° flexion of the lumbar spine was controlled using a manual goniometer, located at the level of ASIS. A belt held the goniometer in place throughout the posture.
- Bending backward (30°): After 5-min rest (same position as rest 2), active 30° extension of the spine was controlled using a manual goniometer, located at the level of ASIS. A belt held the goniometer in place throughout the posture.

To ensure the reproducibility of the measurements, the effect of diurnal variation was minimized by performing the measurements for each participant in the morning.

Once the participant was appropriately positioned, four sites of elastography investigation were identified, on right and left sides of the spine, for the evaluation of PsM stiffness: (1) at the level of the 1st sacral vertebra (S1), 2 cm lateral to the spinous process, in the multifidus muscle; (2) at the level of the 3rd lumbar vertebra (L3), 1–2 cm lateral to the spinous process, in the multifidus; (3) at the level of L3, 1–2 cm lateral to the spinous process in the longissimus; and (4) 5 cm from the spinous process in the iliocostalis. As the lumbar multifidus has different attachments depending on its cranial insertion on the spinous process, multifidus stiffness was studied at both L3 and S1. The spinous process of L4 was first located at the level of the iliac crest by manual palpation. L3 was then manually identified as the spinous process located just above L4, and S1, was identified as the spinous process located two vertebrae below L4. The correct position of the spinal level was then confirmed by B-mode analysis.

Each posture lasted 5 min, thus, session 1 lasted 30 min and session 2 lasted 45 min per participant.

Before the beginning of each session, anatomical landmarks were manually assessed on two orthogonal planes to ensure proper location of the probe above the muscle. The transverse plane allowed the three muscles in the paraspinal compartment to be discriminated. At S1, the paraspinal compartment is made up of the multifidus only (Fig. 2A). At L3, the multifidus has a triangular shape, medially limited by the cortical bone of the spinous process (hyperechogenic), laterally by the epimysial fascia of the multifidus and the fat-filled intermuscular space between the multifidus and the longissimus (hyperechogenic), and inferiorly by the cortical bone of the mamillary process (hyperechogenic; Fig. 3A). The longissimus was located superior and lateral to the multifidus. Under the erector spinae aponeurosis (ESA) and the posterior layer of the TLF (pTLF), the muscle bellies of the erector spinae (longissimus and iliocostalis) are separated by the intermuscular aponeurosis and by a fat-filled intermuscular space (hyperechogenic). After the muscular target (multifidus at S1, multifidus at L3, longissimus or iliocostalis) was identified on the transverse plane, the longitudinal plane was used to locate the section on which stiffness was to be measured and confirm the appropriate alignment of the probe with respect to the muscle fibres by tracing several fascicles without interruption across the B-mode image. At S1, the curve of the cortical bone of the lateral sacral crest served as anatomical landmark for the multifidus at S1 on section 1 (Fig. 2B). Stiffness of the longissimus and the multifidus at L3 was measured within the same section 2 (Fig. 3B). In section 2, the multifidus was bordered by the cortical bone of the mamillary process (hyperechogenic) and the middle layer of the TLF (imperceptible); it was separated from the longissimus by the horizontal fat-filled intermuscular space (hyperechogenic). Section 3 was located in the middle of the iliocostalis, 5 cm from the spinous process (Fig. 3C). Overall, measurements were performed on three longitudinal sections, which were marked on the skin bilaterally with a waterproof felt-tip pen.

After each acquisition, a careful visual inspection of the stiffness map was performed for a global analysis of artefacts, spatial distribution of stiffness, and quality of results. Regional analysis was performed within a 10-mm diameter circular region of interest (ROI) with Aixplorer® analysis software Q-Box. ROIs were manually placed 5 mm below the ESA in the multifidus at S1 in section 1 and in the iliocostalis in section 3. In section 2, the ROIs were manually positioned in the multifidus at L3 between the epimysial fascia of the multifidus and the cortical bone of the mamillary process, and in the longissimus between the ESA and the epimysial fascia of the

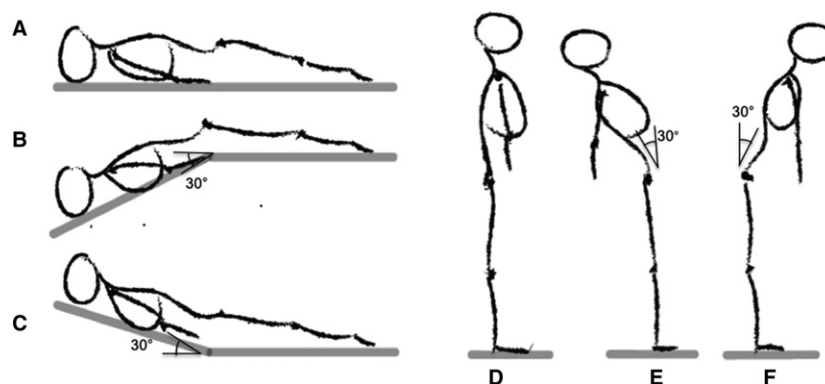
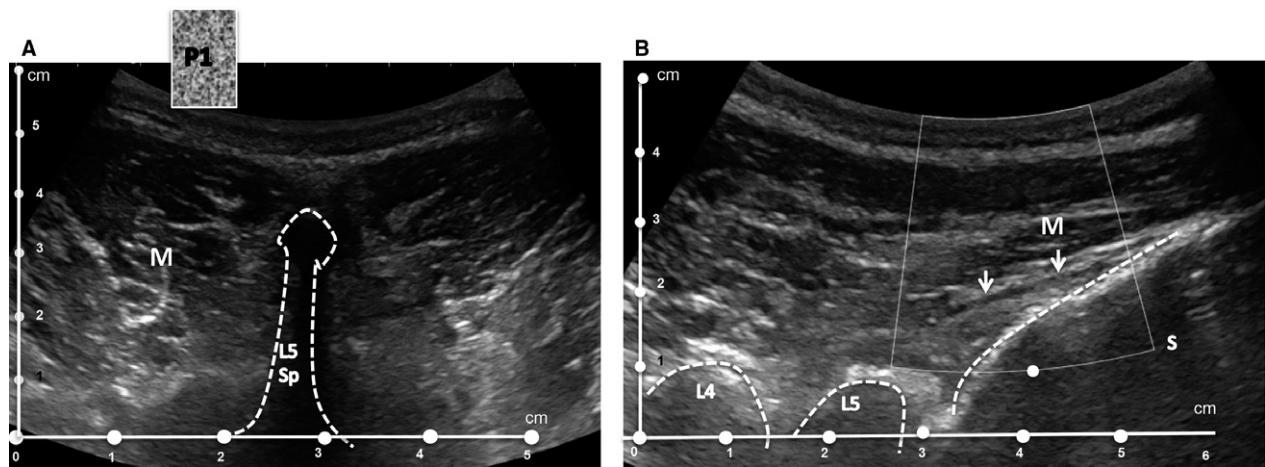
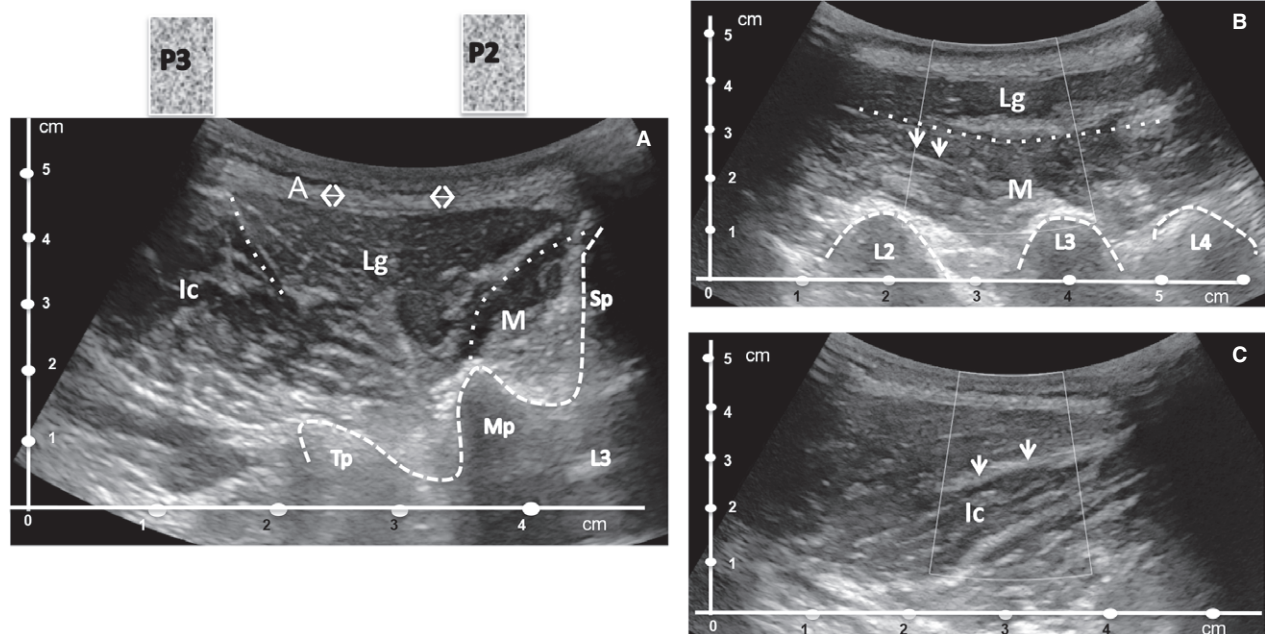


Fig. 1 Illustration of the six postures: (A) rest; (B) passive flexion; (C) passive extension; (D) upright; (E) forward bending; (F) backward bending.



**Fig. 2** Anatomical landmarks on B-mode at S1: (A) transversal plane; (B) longitudinal plane. White arrows show the fibre orientation. The white box indicates the Q-box tool (Aixplorer® analysis software), in which the SWV is recorded. M, multifidus; P1, 1st probe position; S, sacrum; Sp, spinous process.



**Fig. 3** Anatomical landmarks on B-mode at L3. (A) Transversal plane. Double arrows show the ESA and the pTLF. (B,C) Longitudinal plane in the multifidus and longissimus (P2) and in the iliocostalis (P3). The white box indicates the Q-box tool (Aixplorer® analysis software), in which the SWV is recorded. White arrows show the fibre orientation. Lc, iliocostalis; Lg, longissimus; L2, 2nd lumbar vertebrae; L3, 3rd lumbar vertebrae; L4, 4th lumbar vertebrae; M, multifidus; Mp, mammillary process; P2, 2nd probe position; P3, 3rd probe position; Sp, spinous process; Tp, transverse process.

multifidus. Care was taken to avoid any inclusion of ESA, pTLF, fat, vessel or muscle located close to the vertebra in the ROI, as this can affect the measurement outcomes (Ewertsen et al. 2016).

## Statistical analysis

### Reproducibility

Saturated data ( $n = 9$ , image = 54, i.e. for the longissimus during bending forward) were excluded from the statistical analysis. For

each posture and each muscle, reliability between three repeated measures and cross-session reproducibility were evaluated by using intra-class correlation (ICC, 95% confidence intervals). ICC was qualified as poor when  $<0.40$ ; fair when between 0.40 and 0.59; good when between 0.60 and 0.74; and excellent when between 0.75 and 1.00.

Mean stiffness values were used for the next steps. The normality of the data was tested using Shapiro–Wilk's test and analysed with a histogram method. As four variables (mean stiffness values for the multifidus at S1 in passive extension, the multifidus at S1 in bending



backward, the multifidus at L3 in passive extension, and the multifidus at L1 in bending backward) were not normally distributed, nonparametric tests were used. A Wilcoxon matched-paired signed-rank test was performed to compare the SWV between rest postures and the SWV between the left and right muscles. In the absence of any significant differences between sides, left and right results were pooled. For each posture, the Wilcoxon matched-paired signed-rank test was performed to compare the SWV between the multifidus at L3 and at S1.

The one-way analysis of variance (one-way ANOVA; stiffness by muscle and stiffness by posture) was used to determine the intra- and intermuscular difference according to posture and to determine the effect of posture. When the test was significant ( $P < 0.05$ ), *post hoc* Tukey testing was performed. Note that one-way ANOVA requires normality in the dataset. In our study, most of the variables were normally distributed (24 of 28 measures). We cross-checked the results of ANOVA with the Kruskal–Wallis test; as the results were the same, we decided to present results of ANOVA for consistency and clarity in the text. Boxplots illustrate intra- and interstiffness differences with posture.

To determine the magnitude of posture-related stiffness change, the stiffness percentage change between rest and the other postures was defined with the following formulae: percentage change =  $(\text{rest 1} - \text{passive posture})/(\text{rest 1}) \times 100$  and percentage change =  $(\text{rest 2} - \text{active posture})/(\text{rest 2}) \times 100$ , where rest 1, rest 2, passive postures, and active postures are defined in the experimental protocol section.

Statistical analyses were performed with STATA 14 software (StataCorp LP, College Station, TX, USA).  $P$ -values  $< 0.05$  were considered statistically significant.

## Results

On the B-mode image, the orientation of the fibres was clear in the longissimus and the iliocostalis. They were aligned with the longitudinal axis of the muscle belly (Fig. 3B,C). Ultrasound typically reveals muscle fibres, as they are arranged in parallel hypoechoic fascicles and surrounded by echogenic fibro-fatty septa and perimysium. In the longitudinal plane, the perimysium is depicted as multiple parallel lines at an oblique angle with the fascia or the muscle–tendon junction, separated by hypoechoic fascicles. Overall, PsM fibres are parallel to the spinous process line. Anatomical landmarks (bone, fascia, fibre direction) were easily identifiable on B-mode image. Although the delineation of the multifidus fibres was difficult because of the overlap of differently oriented fibres, muscle fibres were globally found oriented parallel to the probe position (Figs 4 and 5).

Shear wave elastography elastograms revealed two distinct mechanical patterns. In most cases, the stiffness was homogeneous over a given muscle. For some participants, pTLF and ESA were responsible for an increase in stiffness in the superficial layer of the underlying muscles (longissimus and multifidus at S1), which we call the ‘fascia effect.’ Postures in which the fascia effect appeared, differed among individuals (Figs 4B,F and 5A–D). Small artefacts were observed near the lamina and the transverse processes of

the vertebra (Fig. 5B). During upright and forward bending postures, elastograms could not be fully reconstructed over the targeted field of view. In nine individuals, the elastogram was totally saturated in the longissimus during forward bending. These data were not included in the statistical analysis.

## Reliability

Intra-class correlation showed good to excellent agreement between the three measurements with the following exceptions: the multifidus at S1 during forward bending [right ICC: 0.46 (–0.33 to 0.81);  $P = 0.09$ ; left ICC: 0.20 (–1.04 to 0.73);  $P = 0.30$ ]; the left multifidus at L3 [ICC: –0.06 (–1.52 to 0.64);  $P = 0.52$ ]; and the left iliocostalis during backward bending [ICC: 0.48 (–0.15 to 0.81);  $P = 0.06$ ] and passive extension [ICC: 0.11 (–1.22 to 0.67);  $P = 0.39$ ; Table 1]. *Post hoc* power analysis showed that we had sufficient power to detect the differences between male and female. Inter-session reproducibility at rest was poor in the multifidus at S1 [ICC: 0.28 (–0.49 to 0.65);  $P = 0.19$ ], fair in the multifidus at L3 [ICC: 0.56 (0.08–0.80);  $P < 0.01$ ] and in the iliocostalis [ICC: 0.47 (–0.07 to 0.75);  $P = 0.04$ ]. Stiffness was significantly higher at rest in the longissimus in rest 1 than in rest 2 ( $P = 0.01$ ). No other day-to-day differences were observed in the other muscles.

## Intra- and intermuscular comparisons

Stiffness was significantly greater in the multifidus at S1 than in the multifidus at L3 during passive extension ( $P < 0.01$ ), upright position ( $P < 0.01$ ), forward bending ( $P = 0.02$ ), and backward bending ( $P = 0.05$ ; Table 2, Fig. 6).

## Interaction between muscles and posture

With respect to rest, the muscle stiffness increased in almost all conditions except passive extension. The ANOVA showed significant higher stiffness during upright position and forward bending compared with all passive postures, during upright posture compared with forward bending, and during upright position and forward bending compared with backward bending [ $F(\text{multifidus at S1}) = 101.83$ ,  $F(\text{multifidus at L3}) = 124.3$ ,  $F(\text{longissimus}) = 59.7$ ,  $F(\text{iliocostalis}) = 92.98$ ;  $P < 0.01$ ]. Passive extension was responsible for increased stiffness in the multifidus at S1 and the iliocostalis, and for decreased stiffness in the multifidus at L3 and the longissimus.

At rest, stiffness was significantly greater in the longissimus than in the iliocostalis [ $F = 5.02$ ,  $P < 0.01$  (rest 1) and  $F = 4.07$ ,  $P < 0.01$  (rest 2)]. In passive flexion, stiffness in the multifidus at S1 was significantly greater than that in the iliocostalis ( $F = 3.4$ ,  $P = 0.02$ ), and in passive extension, stiffness was significantly greater in the multifidus at S1 than in

the multifidus at L3 ( $F = 4.04$ ,  $P < 0.01$ ). In forward bending, iliocostalis stiffness was significantly lower than that in the other muscles ( $F = 7.88$ ,  $P < 0.01$ ). In backward bending, muscle stiffness was not significantly different between muscles ( $F = 2.49$ ,  $P = 0.0644$ ).

## Discussion

Shear wave elastography was successively performed in PsM. From the SWV recorded in PsM over 16 volunteers, we found that (1) under certain controlled conditions, SWE had good to excellent reliability; (2) PsM stiffness exhibited large interindividual variability and large day-to-day variability; and (3) SWE was sensitive to postures, both passive and active. Noticeably, the muscle shear elastic modulus was significantly greater during the upright position and forward bending than passive postures and backward bending.

## Stiffness reliability

In the longissimus and the iliocostalis, intra-session agreement was good to excellent, whereas it was poor or fair during active postures in the multifidus. Previous studies on trunk muscles reported good to excellent intra-session reliability except in the rectus abdominis (MacDonald et al. 2015; Moreau et al. 2016). Results from our studies dealing with trunk muscle stiffness reliability were slightly lower than those reported in studies on appendicular and superficial muscle stiffness (Lacourpaille et al. 2015; Umehara et al. 2015; Moreau et al. 2016). We hypothesized that due to the complex anatomy and number of joints that can influence the length of the muscles tested here, the ability to be in the same relative scanning position can be compromised between repetitions. This will likely modify the reliability of the stiffness measurement. Moreover, the depth and the stretching/contraction of muscles, which may differ slightly

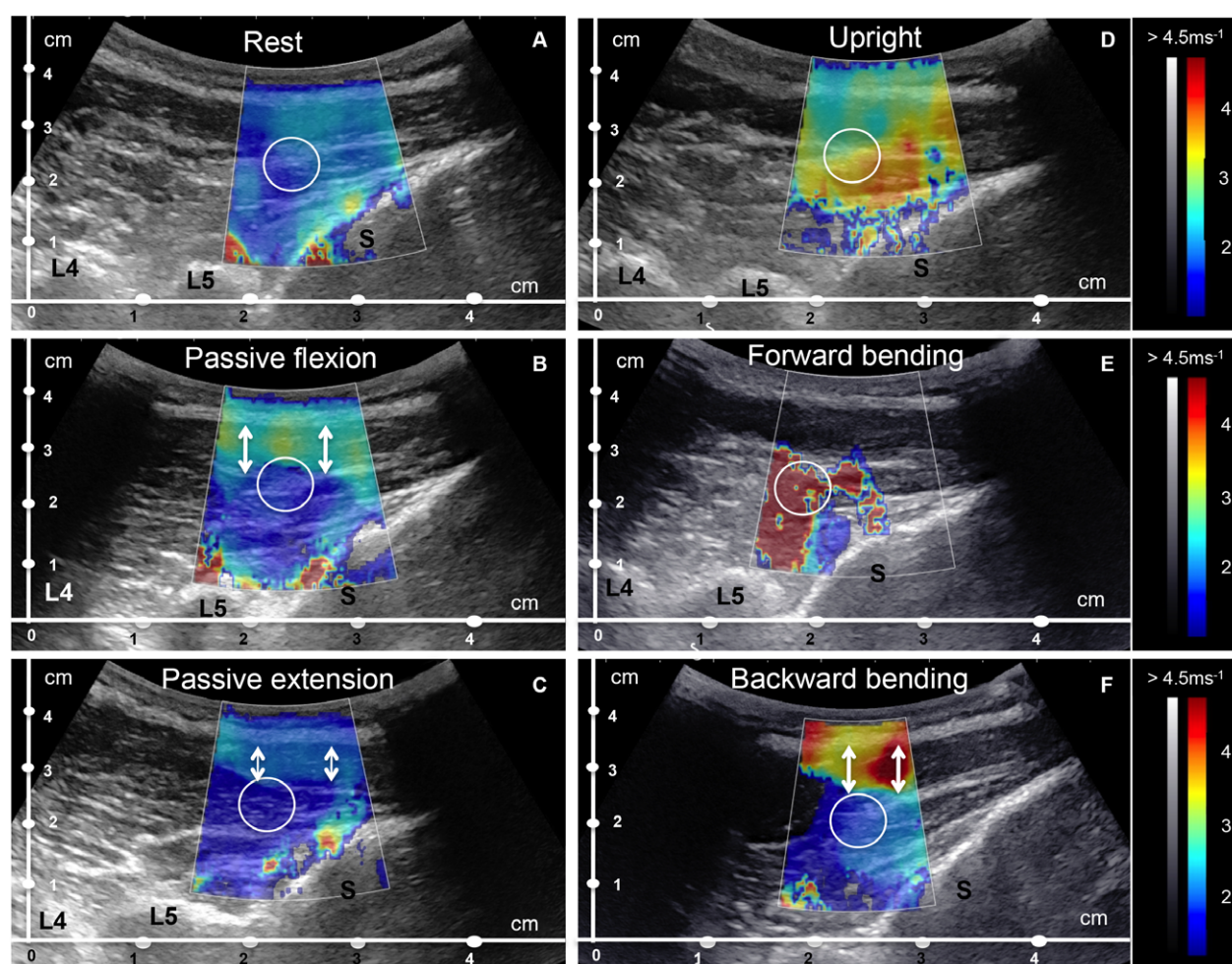


**Fig. 4** Ultrasound image of the left multifidus at S1 with B-mode imaging and with elastographic image overlaid. Stiffness increased in upright posture and forward bending. Stiffness was higher (warm colours) in the superficial part of the multifidus and in the ESA than in the deepest part of the multifidus (cold colours) in passive flexion and backward bending, which we called the fascia effect (double arrows). The white circle showed the ROI position. L4, 4th lumbar vertebrae; L5, 5th lumbar vertebrae; S, sacrum.



between measurements, can also influence the stiffness measurement reliability. Forward bending posture, which is related to both stretching and contraction of the multifidus, presented lower stiffness reproducibility than other postures. Previous studies on appendicular muscles reported lower stiffness reliability during stretching and contraction than at rest (Bouillard et al. 2012b; Kot et al. 2012; Carpenter et al. 2015; Dubois et al. 2015). Moreover, because of gravity and upper bodyweight, keeping one's balance during forward bending yielded little rocking movements with every participant. When applied to the scale of short segmental fascicles of the multifidus, such small motions may (1) alter the stretching and the neuromuscular response of the multifidus, and (2) degrade the SWE outcomes with additional motion artefacts.

In forward bending posture, the elastogram was entirely saturated in the longissimus in nine participants. This finding means that the muscle SWV of these individuals exceeded the range of values measurable by the ultrasound

scanner (Nordez & Hug, 2010). For rigid tissues, SW may propagate too fast, with a velocity  $> 16 \text{ m s}^{-1}$ , to be properly quantified by SWE in the current version of the system. Thus, for the specific measurement case in the contracted longissimus, the outcomes of nine participants (55% of the participants) had to be removed from the analysis.

### Inter-session stiffness reproducibility

The reproducibility from one session to another was not high and rather poor in the longissimus. Previous studies dealing with trunk muscles, in particular abdominal wall muscles, also presented poorer day-to-day reproducibility than in appendicular muscles, as well as significant inter-session differences in the rectus abdominis (Moreau et al. 2016; Tran et al. 2016). Poor stiffness reproducibility may be related to daily variations in the participants' personal and professional occupations; they exerted themselves and their trunk muscles and fascia at different intensities and in a

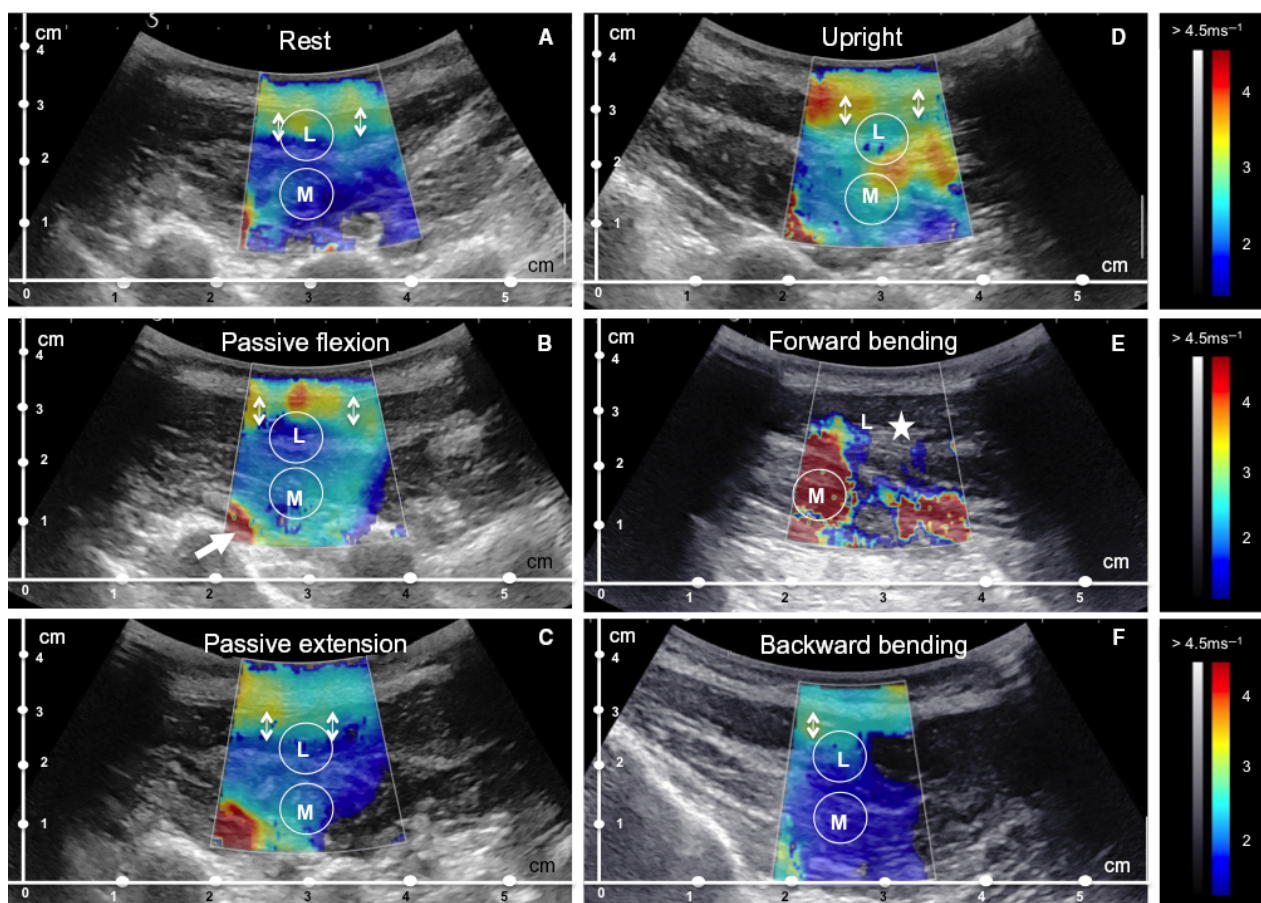


**Fig. 5** Ultrasound image of the left multifidus at L3 and the longissimus with B-mode imaging and with elastographic image overlaid. Stiffness increased in upright posture and forward bending. The white circles showed ROI position. The elastogram was totally saturated in the longissimus during forward bending (white star). Stiffness was higher (warm colours) in the superficial part of the longissimus and in the ESA than in the deepest part of the longissimus (cold colours), which we called the fascia effect (double arrows). Small artefacts were observed near the lamina and the transverse processes of the vertebra [white arrow (B)]. L, longissimus; M, multifidus.

**Table 1** Reliability of shear wave velocity measurements.

Muscle	Posture	Left side				Right side			
		ICC average	95% CI		P-value	ICC average	95% CI		P-value
Multifidus (S1)	Rest 1	0.76	0.45	0.91	$< 10^{-3}$	0.94	0.86	0.98	$< 10^{-3}$
	Passive flexion	0.90	0.76	0.96	$< 10^{-3}$	0.94	0.86	0.97	$< 10^{-3}$
	Passive extension	0.95	0.90	0.98	$< 10^{-3}$	0.97	0.93	0.99	$< 10^{-3}$
	Rest 2	0.81	0.54	0.93	$< 10^{-3}$	0.71	0.29	0.90	$< 10^{-3}$
	Upright	0.90	0.76	0.96	$< 10^{-3}$	0.90	0.77	0.97	$< 10^{-3}$
	Bending forward	0.20	-1.04	0.73	0.30	0.46	-0.33	0.81	0.09
	Bending backward	0.85	0.64	0.95	$< 10^{-3}$	0.91	0.79	0.97	$< 10^{-3}$
Multifidus (L3)	Rest 1	0.53	-0.12	0.83	0.04	0.86	0.67	0.95	$< 10^{-3}$
	Passive flexion	0.93	0.85	0.97	$< 10^{-3}$	0.83	0.61	0.93	$< 10^{-3}$
	Passive extension	0.91	0.79	0.97	$< 10^{-3}$	0.84	0.65	0.94	$< 10^{-3}$
	Rest 2	0.92	0.81	0.97	$< 10^{-3}$	0.84	0.63	0.94	$< 10^{-3}$
	Upright	0.93	0.83	0.97	$< 10^{-3}$	0.89	0.75	0.96	$< 10^{-3}$
	Bending forward	0.87	0.69	0.96	$< 10^{-3}$	0.74	0.31	0.91	$< 10^{-3}$
	Bending backward	-0.06	-1.52	0.64	0.52	0.80	0.48	0.94	$< 10^{-3}$
Longissimus	Rest 1	0.91	0.79	0.97	$< 10^{-3}$	0.76	0.43	0.91	$< 10^{-3}$
	Passive flexion	0.71	0.33	0.89	$< 10^{-3}$	0.93	0.83	0.97	$< 10^{-3}$
	Passive extension	0.91	0.78	0.97	$< 10^{-3}$	0.86	0.67	0.95	$< 10^{-3}$
	Rest 2	0.92	0.80	0.97	$< 10^{-3}$	0.84	0.63	0.94	$< 10^{-3}$
	Upright	0.92	0.82	0.97	$< 10^{-3}$	0.89	0.67	0.95	$< 10^{-3}$
	Bending forward	0.89	0.65	0.98	$< 10^{-3}$	0.76	0.28	0.94	0.01
	Bending backward	0.56	-0.09	0.86	0.04	0.88	0.70	0.96	$< 10^{-3}$
Iliocostalis	Rest 1	0.80	0.54	0.93	$< 10^{-3}$	0.86	0.68	0.95	$< 10^{-3}$
	Passive flexion	0.79	0.51	0.92	$< 10^{-3}$	0.73	0.37	0.90	$< 10^{-3}$
	Passive extension	0.11	-1.22	0.67	0.39	0.84	0.63	0.94	$< 10^{-3}$
	Rest 2	0.71	0.35	0.89	$< 10^{-3}$	0.85	0.66	0.95	$< 10^{-3}$
	Upright	0.83	0.61	0.94	$< 10^{-3}$	0.92	0.80	0.97	$< 10^{-3}$
	Bending forward	0.79	0.50	0.93	$< 10^{-3}$	0.61	-0.01	0.87	0.03
	Bending backward	0.48	-0.15	0.81	0.06	0.83	0.59	0.94	$< 10^{-3}$

95% CI, 95% confidence intervals; ICC, intra-class correlation coefficient.

**Table 2** Mean shear wave velocity (standard deviation) in  $\text{m s}^{-1}$  and percentage change from rest for the six postures.

	Multifidus S1	Multifidus L3	Longissimus	Iliocostalis
Session 1				
Rest	2.24 (0.45)	2.21 (0.40)	2.48 (0.55)	2.06 (0.34)
Passive flexion	2.61 (0.49)	2.41 (0.46)	2.53 (0.52)	2.27 (0.38)
	+17 (4.5)%	+9 (2.8)%	+2 (0.2)%	+10 (3.4)%
Passive extension	2.50 (0.70)	2.09 (0.52)	2.39 (0.55)	2.17 (0.29)
	+12 (3.1)%	-5 (2.0)%	-4 (2.7)%	+5 (2.0)%
Session 2				
Rest	2.15 (0.26)	1.99 (0.34)	2.22 (0.34)	2.00 (0.25)
Upright	4.17 (1.08)*	3.01 (0.77)*	3.32 (1.03)*	2.67 (0.71)*
	+94 (35.5)%	+51 (24.0)%	+50 (17.7)%	+33 (9.8)%
Bending forward	5.19 (0.43)*,†	5.58 (0.91)*,†	5.36 (0.91)*,†	5.57 (0.92)*,†
	+141 (47.3)%	+180 (49.2)%	+141 (39.9)%	179 (43.6)%
Bending backward	2.46 (0.59)	2.21 (0.71)	2.25 (0.33)	2.09 (0.33)
	+14 (6.2)%	+11 (4.1)%	+1 (0.8)%	+5 (1.7)%

\*Significantly higher ( $P < 0.05$ ) than rest, passive posture, and bending backward.†Significantly higher ( $P < 0.05$ ) compared with upright.



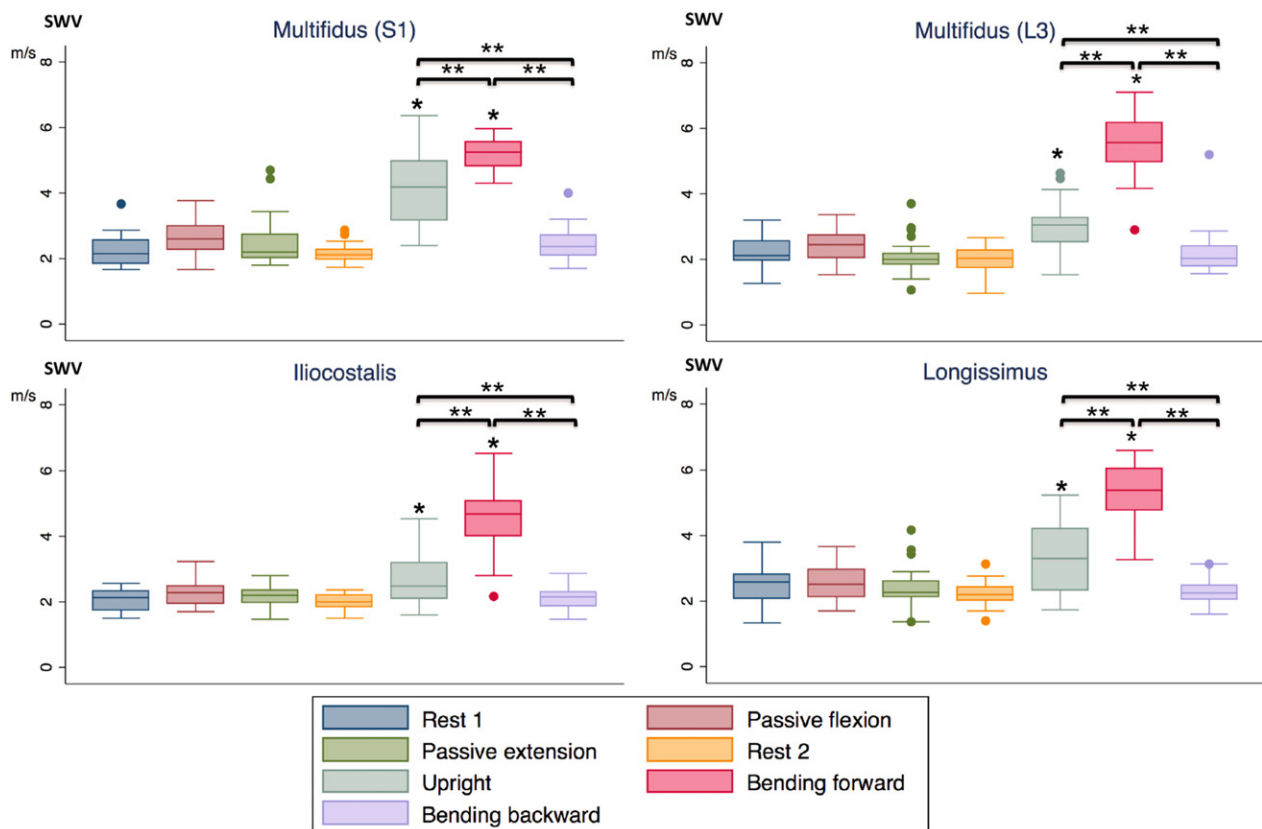


**Fig. 6** Boxplot showing intra- and intermuscular differences. SWV, shear wave velocity. \* Significantly higher ( $P < 0.05$ ) than rest, passive posture, and bending backward. \*\* Significant difference between muscles ( $P < 0.05$ ).

variety of ways from day-to-day (bearing heavy loads, upright positions, seating positions). Moreover, to the best of our knowledge, little is known about daily changes in muscle stiffness. *In vivo* and *ex vivo* testing on the lumbar spine revealed significant diurnal changes in the spinal range of motion related to stiffness changes in disc and ligaments of the neural arch caused by changes in disc water content, disc swelling pressure, and compressive stiffness, in particular after heavy loading (Adams et al. 1987, 1990). Similar trends could be observed in PsM intimately connected to the vertebral column and enclosed in an inextensible osteo-fibrous compartment.

### Spatial variability of stiffness

Few data are available in the literature to which the outcomes reported here could be compared. Nevertheless, in general, our results are fairly consistent with previously reported works on PsM measured either at other spinal levels or with other imaging methods. For example, at rest, Dieterich et al. (2017) presented the median shear modulus at 14.9 kPa (i.e.  $3.86 \text{ m s}^{-1}$ ) in the multifidus at the cervical level. In another study, Moreau and colleagues obtained 13.86 kPa (i.e.  $3.72 \text{ m s}^{-1}$ ) at L2–L3, and 22.76 kPa (i.e.  $4.77 \text{ m s}^{-1}$ ) in the multifidus at L3–L4 and Creze et al.

reported 6.9 kPa (i.e.  $2.62 \text{ m s}^{-1}$ ) in the longissimus, 4.9 kPa ( $2.21 \text{ m s}^{-1}$ ) in the iliocostalis, and 5.4 kPa (i.e.  $2.32 \text{ m s}^{-1}$ ) in the multifidus at L3 (Moreau et al. 2016; Creze et al. 2017).

According to Moreau et al. (2016) significant intramuscular differences are to be expected in the multifidus. The multifidus at S1 has a larger cross-sectional area than the multifidus has at L3. It is covered by ESA and pTLF only, and fascicles have a larger angulation with the spinous process line than they do at L3. Muscle stiffness inhomogeneity has already been observed between the proximal and distal parts and between the surface and the depth of the appendicular muscles. Similar structural and functional organization were observed in the muscle (Nordez & Hug, 2010; Lacourpaille et al. 2012; Eby et al. 2015; Hatta et al. 2016a; Le Sant et al. 2017).

The dispersion of individual muscle stiffness values around the mean was high, in particular during upright and forward bending postures. This result may indicate differences in stretch tolerance and in neuromuscular activity (Le Sant et al. 2017). Moreover, muscle tissue has great plasticity in response to functional demands such as changes in neuromuscular activity or mechanical loading. The history of the muscle preceding the examination, for a period of hours to years, conditions the type and density of muscular

fibres, hydration, and biochemical state (Frontera & Ochala, 2015).

Shear wave elastography revealed two stiffness patterns in the multifidus at S1 and the longissimus: (1) stiffness distribution was uniform between the superficial and deep layers of the muscles, and (2) stiffness was greater in the superficial layer of longissimus and multifidus at S1, under the ESA and the TLF, which we called the fascia effect (Gatton et al. 2010). Similar stiffness patterns were observed in the tibialis anterior muscle, where the cruralis fascia was responsible for a similar fascia effect (Koo et al. 2014). This effect might be related to the singular anatomy of the longissimus near the myoaponeurotic junction with the ESA and to the effect of compression of the pTLF. Part of the muscle located in the vicinity of the myoaponeurotic junction is an atypical region made of sarcolemmal invaginations interspersed with bundles of collagen fibres appearing as finger-like processes (Knudsen et al. 2015). Such a muscle structure might explain why stiffness significantly increases within only a few centimetres of the myoaponeurotic junction (Yoshitake et al. 2014; Le Sant et al. 2017). Moreover, the pTLF has been postulated to act as a retinaculum that covers and gently presses the PsM down, in particular the outer longissimus and the multifidus at S1 (Bogduk & Macintosh, 1984). By comparing muscle stiffness with and without skin and fascia in human cadavers using SWE, some investigators showed that skin and fascia contributed to increased muscular stiffness in the legs (Koo et al. 2014; Yoshitake et al. 2014). As found in a previous study, the fascia effect was inconstant. Variability of this effect could be related to interindividual variability of fascial thickness, fibrosity, stiffness, and the tensile effect of muscle attachments on the pTLF and ESA (Barker et al. 2004; Kramer et al. 2004; Langevin et al. 2011; Pavan et al. 2014; Yoshitake et al. 2014).

In contrast to the pTLF, which is a mesh of differently oriented fibres, the ESA comprises longitudinal fibres arranged in fascicles, more or less dense according to the participant's anatomy, which create interfascicular spaces (longitudinal fenestration; Creze et al. 2017). Indeed, in some cases, a small tilt of the probe opened an acoustic window that circumvented the fascia effect. In addition, we cannot exclude the possibility that hard fascia and ESA generated measurement artefacts that led to increased stiffness in the superficial part of the muscles. Given the inhomogeneity of the spatial distribution of stiffness in the muscle, the stiffness value highly depends on the location and size of the ROI. It affects the measurement reproducibility (Ates et al. 2015; Ewertsen et al. 2016).

### Posture-related changes of muscle elasticity

Different stiffness changes were identified between PsM in relation to posture (Creze et al. 2018a). According to Chan et al. (2012), stiffness increased in their study from lying to

standing postures except when the participants were bending backward. Using strain elastography, they demonstrated that Young's modulus,  $E$ , increased from the prone to the upright position and continued increasing when the participants bent forward at 25° and 45°. The multifidus stiffness simply increases with postural demand. Increased stiffness with upright and forward bending postures can be explained by the cumulative effect of many biomechanical changes, such as increased intramuscular pressure, tension, compressive effect of the pTLF, and neuromuscular activity (Donisch & Basmajian, 1972; Peach et al. 1998). Previous studies using SWE on appendicular muscles reported a positive and linear relationship between stiffness and muscle force (Nordez & Hug, 2010; Hug et al. 2015). In healthy participants, PsM are almost electrically silent during upright standing and backward bending, but neuromuscular activity increases during the initial phase of active flexion related to active force (Donisch & Basmajian, 1972; Peach et al. 1998). SWE failed to detect SW propagation in the longissimus (saturation of the elastogram) in forward bending posture related to muscular stiffness that was greater than that measurable with the settings used in this study. Calculation of the overall average values excluded nine participants in whom longissimus mean stiffness was underestimated in bending forward, which is much higher than stiffness in the multifidus and iliocostalis. Such a high stiffness increase in the longissimus might be related to the close relationship between the longissimus, the ESA, and the TLF. During muscle contraction, as muscle generates force and shortens, the aponeurosis stretches, thus its stiffness increases (Gatton et al. 2010). As described earlier, the pTLF also creates an axial force that limits radial expansion of the PsM during contraction, and thus the stiffness in the longissimus increases all the more (Gatton et al. 2010).

### Functional significance

Magnitude of stiffness changes, between postures, differed between the multifidus, the longissimus, and the iliocostalis, suggesting a different biomechanical behaviour of each PsM. For any postures, the longissimus presented the highest stiffness values, which supports permanent stiffness to the spine. The segmental multifidus, which is affixed to the spinal arch, had low stiffness at rest, but it proportionally stiffened more than the other muscles did in most postures, providing strong vertebral joint stabilization. Among the PsM, stiffness of the iliocostalis was the lowest.

PsM are numerous and their highly complex anatomy makes it difficult to model their modes of action. The stabilizing role of the PsM cannot be easily studied by electromyographic (EMG) measurement of the muscles alone. The EMG recording from a muscle indicates the electrical activity of the muscle but does not provide the related quantitative measurement of the muscle force (Fryer et al. 2004a). Furthermore, deep muscles, including the

multifidus, are difficult to reach. PsM are unsheathed in an inextensible osteo-fascial compartment. Pressure and stiffness in the compartment ensure clamping of the vertebrae. They create two bone–muscle composite beams that stiffen the spine (Kramer et al. 2004, 2005; Dupeyron et al. 2009). Muscle stiffness is related to (1) muscle active force and muscle activity, (2) muscle passive force and lengthening, and (3) external tensional influence. The conjunction of the various functions of the paraspinal compartment during spine motion and posture is integrated by SWE. Therefore, each contribution cannot be differentiated by the measurement of stiffness.

Several investigators have suggested that alteration of passive and active tissues stiffness of the lumbar region may lead to spinal instability, increase spinal stiffness and cause low back pain (Panjabi, 1992). In the field of spinal surgery and rehabilitation, the preservation of the ‘elastic equilibrium’ of the spine, that is, the lumbar spine posture of least stiffness during daily life activity, is critical to reduce and prevent LBP (Scannell & McGill, 2003). The neutral zone is the range of lumbar positions of least tissue strain (Scannell & McGill, 2003). *In vivo* motion track systems are used to assess the spinal stiffness and the neutral zone, but they do not provide quantitative stiffness changes and they do not distinguish the involvement of any specific tissue. Moreover, these techniques are hard to achieve in clinical practice and are rarely applied. Therefore, SWE, being indicative of posture-related stiffness changes of the PsM, could help clinicians to identify this neutral zone accurately, thus improving the management of LBP.

Shear wave elastography revealed a fascia effect in some participants in different postures. An increase in fascia in the superficial part of the muscles might predispose an individual to a higher risk of developing chronic compartment syndrome and LBP (Koo et al. 2014). A longitudinal study needs to be done to challenge this hypothesis.

### Limitations

The study has several limitations. First, with the small number of volunteers, the study is subject to individual variation and the interpretation on muscle stiffness is restricted. However, no previous study has analysed the performance of SWE in measuring the stiffness of PsM. In future investigations with larger cohorts, we will aim to confirm the accuracy and precision of SWE. Second, SWE measurements (in particular in the multifidus) have been obtained in a media with superposed fascicles of different orientations (Creze et al. 2017). Therefore, some muscle fibres had an angle up to 20° with the principal axis of the probe, which is known to modify the measured stiffness value (Macintosh et al. 1987; Macintosh & Bogduk, 1991). Muscles can be considered transverse isotropic media, with one main axis (along the fibres). To properly quantify the stiffness along to the fibres, the ultrasonic probe must be aligned with the muscle

fibres, as described by Royer et al. (2011) and Gennisson et al. (2010). Isotropic elastic medium is assumed. Hence, SWV does not allow accurate characterization of the transverse isotropic stiffness of muscle and, as muscle fibres are not generally all aligned, the measurement is a rough average of the anisotropic stiffness moduli. Thirdly, the convex probe, used here and commonly adapted to abdominal organs, does not offer a muscular preset, which would alleviate the measured stiffness saturation in the contracted longissimus. Another probe dedicated to muscle studies will be used in future works. Fourthly, neuromuscular activity was not measured by electromyography during the examination sessions. Electrodes were not placed on the muscles, and proper placement of the ultrasound probe was favoured. However, PsM neuromuscular activity probably explains stiffness changes related to posture (Donisch & Basmajian, 1972; Peach et al. 1998). Further studies are needed to explore the influence of neuromuscular activity on posture-related stiffness. Fifthly, the protocol of the present study could be improved. We chose ASIS as anatomical landmarks to determinate trunk flexion/extension angle in order to reproduce the postures easily in clinical practice. Although the participants were instructed to keep their back straight during the experiment, the lumbar posture was not continuously monitored and lumbar curvature and hip flexion were not assessed. Finally, the stabilization of any postures results from the combination of co-contraction of PsM and the psoas, intra-abdominal pressure, and gluteus maximus contraction (Hodges et al. 2005). Future SWE studies should take into account these co-actors to study spinal postures fully.

### Conclusion

Muscle stiffness, recorded by SWE, is an objective, quantitative, and sensitive biomarker for different postures as long as the measurement and reconstruction conditions are properly controlled. SWE highlighted the different biomechanical behaviour between paraspinal muscles. This work opens the way for pioneering a clinical study on paraspinal muscles and lower back pain with new biophysical insights.

### Acknowledgements

Grant from Société Française de Radiologie – Collège de Radiologie (SFR-CERF).

### Author contributions

Contributions to concept/design: Marie-France Bellin, Olivier Gagey, Marc Soubeyrand, Maud Creze. Acquisition of data: Maud Creze, Marc Soubeyrand. Data analysis/interpretation: Dina Dinova, Laurence Rocher, Maud Creze, Marc Soubeyrand. Drafting of the manuscript: Maud Creze, Jean-Luc Gennisson, Xavier Maître.



## References

- Adams MA, Dolan P, Hutton WC (1987) Diurnal variations in the stresses on the lumbar spine. *Spine (Phila Pa 1976)*, **12**, 130–137.
- Adams MA, Dolan P, Hutton WC, et al. (1990) Diurnal changes in spinal mechanics and their clinical significance. *J Bone Joint Surg Br* **72**, 266–270.
- Akagi R, Tanaka J, Shikiba T, et al. (2015) Muscle hardness of the triceps brachii before and after a resistance exercise session: a shear wave ultrasound elastography study. *Acta Radiol* **56**, 1487–1493.
- Ates F, Hug F, Bouillard K, et al. (2015) Muscle shear elastic modulus is linearly related to muscle torque over the entire range of isometric contraction intensity. *J Electromyogr Kinesiol* **25**, 703–708.
- Barker PJ, Briggs CA, Bogeski G (2004) Tensile transmission across the lumbar fasciae in unembalmed cadavers: effects of tension to various muscular attachments. *Spine (Phila Pa 1976)*, **29**, 129–138.
- Bercoff J, Tanter M, Muller M, et al. (2004) The role of viscosity in the impulse diffraction field of elastic waves induced by the acoustic radiation force. *IEEE Trans Ultrason Ferroelectr Freq Control* **51**, 1523–1536.
- Bogduk N, Macintosh JE (1984) The applied anatomy of the thoracolumbar fascia. *Spine (Phila Pa 1976)*, **9**, 164–170.
- Bouillard K, Nordez A, Hug F (2011) Estimation of individual muscle force using elastography. *PLoS One* **6**, e29261.
- Bouillard K, Hug F, Guevel A, et al. (2012a) Shear elastic modulus can be used to estimate an index of individual muscle force during a submaximal isometric fatiguing contraction. *J Appl Physiol* (1985), **113**, 1353–1361.
- Bouillard K, Nordez A, Hodges PW, et al. (2012b) Evidence of changes in load sharing during isometric elbow flexion with ramped torque. *J Biomech* **45**, 1424–1429.
- Brown SH, McGill SM (2010) The relationship between trunk muscle activation and trunk stiffness: examining a non-constant stiffness gain. *Comput Methods Biomech Biomed Engin* **13**, 829–835.
- Carpenter EL, Lau HA, Kolodny EH, et al. (2015) Skeletal muscle in healthy subjects versus those with GNE-related myopathy: evaluation with shear-wave US – a pilot study. *Radiology* **277**, 546–554.
- Chan ST, Fung PK, Ng NY, et al. (2012) Dynamic changes of elasticity, cross-sectional area, and fat infiltration of multifidus at different postures in men with chronic low back pain. *Spine J* **12**, 381–388.
- Chino K, Takahashi H (2016) Measurement of gastrocnemius muscle elasticity by shear wave elastography: association with passive ankle joint stiffness and sex differences. *Eur J Appl Physiol* **116**, 823–830.
- Colloca CJ, Hinrichs RN (2005) The biomechanical and clinical significance of the lumbar erector spinae flexion-relaxation phenomenon: a review of literature. *J Manipulative Physiol Ther* **28**, 623–631.
- Creze M, Nyangoh Timoh K, Gagey O, et al. (2017) Feasibility assessment of shear wave elastography to lumbar back muscles: a radioanatomic study. *Clin Anat* **30**, 774–780.
- Creze M, Marc S, Long Yue J, et al. (2018a) Magnetic resonance elastography of the lumbar back muscles: a preliminary study. *Clin Anat* **31**, 514–520.
- Creze M, Nordez A, Soubeyrand M, et al. (2018b) Shear wave sonoelastography of skeletal muscle: basic principles, biomechanical concepts, clinical applications, and future perspectives. *Skeletal Radiol* **47**, 457–471.
- Creze M, Soubeyrand M, Nyangoh Timoh K, et al. (2018c) Organization of the fascia and aponeurosis in the lumbar paraspinal compartment. *Surg Radiol Anat* **40**, 1231–1242.
- Dieterich AV, Andrade RJ, Le Sant G, et al. (2017) Shear wave elastography reveals different degrees of passive and active stiffness of the neck extensor muscles. *Eur J Appl Physiol* **117**, 171–178.
- Donisch EW, Basmajian JV (1972) Electromyography of deep back muscles in man. *Am J Anat* **133**, 25–36.
- Dubois G, Kheireddine W, Vergari C, et al. (2015) Reliable protocol for shear wave elastography of lower limb muscles at rest and during passive stretching. *Ultrasound Med Biol* **41**, 2284–2291.
- Dupeyron A, Lecocq J, Vautravers P, et al. (2009) Muscle oxygenation and intramuscular pressure related to posture and load in back muscles. *Spine J* **9**, 754–759.
- Eby SF, Song P, Chen S, et al. (2013) Validation of shear wave elastography in skeletal muscle. *J Biomech* **46**, 2381–2387.
- Eby SF, Cloud BA, Brandenburg JE, et al. (2015) Shear wave elastography of passive skeletal muscle stiffness: influences of sex and age throughout adulthood. *Clin Biomech (Bristol, Avon)* **30**, 22–27.
- Ewertsen C, Carlsen JF, Christiansen IR, et al. (2016) Evaluation of healthy muscle tissue by strain and shear wave elastography – dependency on depth and ROI position in relation to underlying bone. *Ultrasonics* **71**, 127–133.
- Frontera WR, Ochala J (2015) Skeletal muscle: a brief review of structure and function. *Calcif Tissue Int* **96**, 183–195.
- Fryer G, Morris T, Gibbons P (2004a) Paraspinal muscles and intervertebral dysfunction: part one. *J Manipulative Physiol Ther* **27**, 267–274.
- Fryer GM, Morris T, Gibbons P (2004b) Paraspinal muscles and intervertebral dysfunction: part two. *J Manipulative Physiol Ther* **27**, 348–357.
- Gatton ML, Pearcy MJ, Pettet GJ, et al. (2010) A three-dimensional mathematical model of the thoracolumbar fascia and an estimate of its biomechanical effect. *J Biomech* **43**, 2792–2797.
- Gennisson JL, Deffieux T, Mace E, et al. (2010) Viscoelastic and anisotropic mechanical properties of *in vivo* muscle tissue assessed by supersonic shear imaging. *Ultrasound Med Biol* **36**, 789–801.
- Gennisson JL, Deffieux T, Fink M, et al. (2013) Ultrasound elastography: principles and techniques. *Diagn Interv Imaging* **94**, 487–495.
- Hatta T, Giambini H, Hooke AW, et al. (2016a) Comparison of passive stiffness changes in the supraspinatus muscle after double-row and knotless transosseous-equivalent rotator cuff repair techniques: a cadaveric study. *Arthroscopy* **32**, 1973–1981.
- Hatta T, Giambini H, Sukegawa K, et al. (2016b) Quantified mechanical properties of the deltoid muscle using the shear wave elastography: potential implications for reverse shoulder arthroplasty. *PLoS One* **11**, e0155102.
- Hodges PW, Eriksson AE, Shirley D, et al. (2005) Intra-abdominal pressure increases stiffness of the lumbar spine. *J Biomech* **38**, 1873–1880.
- Hug F, Tucker K, Gennisson JL, et al. (2015) Elastography for muscle biomechanics: toward the estimation of individual muscle force. *Exerc Sport Sci Rev* **43**, 125–133.
- Kalimo H, Rantanen J, Viljanen T, et al. (1989) Lumbar muscles: structure and function. *Ann Med* **21**, 353–359.

- Knudsen AB, Larsen M, Mackey AL, et al. (2015) The human myotendinous junction: an ultrastructural and 3D analysis study. *Scand J Med Sci Sports* **25**, e116–e123.
- Koo TK, Guo JY, Cohen JH, et al. (2014) Quantifying the passive stretching response of human tibialis anterior muscle using shear wave elastography. *Clin Biomech (Bristol, Avon)* **29**, 33–39.
- Koppenhaver S, Kniss J, Lilley D, et al. (2018) Reliability of ultrasound shear-wave elastography in assessing low back musculature elasticity in asymptomatic individuals. *Electromyogr Kinesiol* **39**, 49–57.
- Kot BC, Zhang ZJ, Lee AW, et al. (2012) Elastic modulus of muscle and tendon with shear wave ultrasound elastography: variations with different technical settings. *PLoS One* **7**, e44348.
- Kramer M, Volker HU, Weikert E, et al. (2004) Simultaneous measurement of intramuscular pressure and surface electromyography of the multifidus muscle. *Eur Spine J* **13**, 530–536.
- Kramer M, Dehner C, Hartwig E, et al. (2005) Intramuscular pressure, tissue oxygenation and EMG fatigue measured during isometric fatigue-inducing contraction of the multifidus muscle. *Eur Spine J* **14**, 578–585.
- Lacourpaille L, Hug F, Bouillard K, et al. (2012) Supersonic shear imaging provides a reliable measurement of resting muscle shear elastic modulus. *Physiol Meas* **33**, N19–N28.
- Lacourpaille L, Nordez A, Hug F, et al. (2014) Time-course effect of exercise-induced muscle damage on localized muscle mechanical properties assessed using elastography. *Acta Physiol (Oxf)* **211**, 135–146.
- Lacourpaille L, Hug F, Guevel A, et al. (2015) Non-invasive assessment of muscle stiffness in patients with Duchenne muscular dystrophy. *Muscle Nerve* **51**, 284–286.
- Langevin HM, Fox JR, Koptiuch C, et al. (2011) Reduced thoracolumbar fascia shear strain in human chronic low back pain. *BMC Musculoskelet Disord* **12**, 203.
- Le Sant G, Nordez A, Andrade R, et al. (2017) Stiffness mapping of lower leg muscles during passive dorsiflexion. *J Anat* **230**, 639–650.
- Levinson SF, Shinagawa M, Sato T (1995) Sonoelastic determination of human skeletal muscle elasticity. *J Biomech* **28**, 1145–1154.
- Mabit CPFGJC, Rabischong P (1996) La stabilisation musculaire du rachis. *Rev Fr Méc* **3**, 169–177.
- MacDonald D, Wan A, McPhee M, et al. (2015) Reliability of abdominal muscle stiffness measured using elastography during trunk rehabilitation exercises. *Ultrasound Med Biol* **42**, 1018–1025.
- Macintosh JE, Bogduk N (1991) The attachments of the lumbar erector spinae. *Spine (Phila Pa 1976)* **16**, 783–792.
- Macintosh JE, Bogduk N, Gracovetsky S (1987) The biomechanics of the thoracolumbar fascia. *Clin Biomech (Bristol, Avon)* **2**, 78–83.
- Moreau B, Vergari C, Gad H, et al. (2016) Non-invasive assessment of human multifidus muscle stiffness using ultrasound shear wave elastography: a feasibility study. *Proc Inst Mech Eng H* **230**, 809–814.
- Masaki M, Aoyama T, Murakami T, et al. (2017) Association of low back pain with muscle stiffness and muscle mass of the lumbar back muscles, and sagittal spinal alignment in young and middle-aged medical workers. *Clin Biomech (Bristol, Avon)* **49**, 128–133.
- Nordez A, Hug F (2010) Muscle shear elastic modulus measured using supersonic shear imaging is highly related to muscle activity level. *J Appl Physiol (1985)* **108**, 1389–1394.
- Panjabi MM (1992) The stabilizing system of the spine. Part I. Function, dysfunction, adaptation, and enhancement. *J Spinal Disord* **5**, 383–389.
- Pavan PG, Stecco A, Stern R, et al. (2014) Painful connections: densification versus fibrosis of fascia. *Curr Pain Headache Rep* **18**, 441.
- Peach JP, Sutarno CG, McGill SM (1998) Three-dimensional kinematics and trunk muscle myoelectric activity in the young lumbar spine: a database. *Arch Phys Med Rehabil* **79**, 663–669.
- Rabischong P, Avril J (1965) Biomechanical role of the bone-muscle composite beams. *Rev Chir Orthop Reparatrice Appar Mot* **51**, 437–458.
- Royer D, Genisson J, Deffieux T, et al. (2011) On the elasticity of transverse isotropic soft tissues (L). *J Acoust Soc Am* **129**, 2757–2760.
- Scannell JP, McGill SM (2003) Lumbar posture—should it, and can it, be modified? A study of passive tissue stiffness and lumbar position during activities of daily living. *Phys Ther* **83**, 907–917.
- Tran D, Podwojewski F, Beillas P, et al. (2016) Abdominal wall muscle elasticity and abdomen local stiffness on healthy volunteers during various physiological activities. *J Mech Behav Biomed Mater* **60**, 451–459.
- Umehara J, Ikezoe T, Nishishita S, et al. (2015) Effect of hip and knee position on tensor fasciae latae elongation during stretching: An ultrasonic shear wave elastography study. *Clin Biomech (Bristol, Avon)* **30**, 1056–1059.
- Willard FH, Vleeming A, Schuenke MD, et al. (2012) The thoracolumbar fascia: anatomy, function and clinical considerations. *J Anat* **221**, 507–536.
- Yoshitake Y, Takai Y, Kanehisa H, et al. (2014) Muscle shear modulus measured with ultrasound shear-wave elastography across a wide range of contraction intensity. *Muscle Nerve* **50**, 103–113.

## Supporting Information

Additional Supporting Information may be found in the online version of this article:

**Fig. S1.** Photographs of the six postures.